ROMANIAN JOURNAL OF INFORMATION SCIENCE AND TECHNOLOGY
Volume 19, Number 3, 2016, 213–225

Backscattering Modulators for UWB Antenna Measurement

V. Buiculescu and I. Giangu

National Institute for Research and Development in Microtechnologies- IMT, 126A (32B) Erou Iancu Nicolae, 077190 Bucharest, Romania
Email: valentin.buiculescu@imt.ro, ioana.giangu@imt.ro

Abstract. Signal backscattering (BS) methods are normally used for gain and radiation pattern measurements of small antennas, mainly due to reduced disturbance from RF feeding cables. Most chipless RFIDs are based on passive structures with broadband, multiple resonances, therefore UWB antennas are best suited for these RFID applications. However, bandwidth of small antennas used in most RFID applications is inherently narrow, hence regular BS modulators used for their characterization work within limited bandwidths. A broadband BS modulator solution is proposed in this paper for covering non-standard and ultra wideband (UWB) antenna measurements. The basic component of this BS modulator can be any monolithic integrated single-pole double through (SPDT) switch with low current consumption and control voltages; both CMOS and pHEMT devices are suitable for this application. A bistatic arrangement provides improved measurement accuracy due to constant coupling factor between transmitting and receiving antennas placed in stationary positions. About 11 μW power consumption from a single 3 V battery was measured for the complete UWB BS modulator, therefore long term antenna characterization with 0.004 dB/day accuracy was possible.

Keywords: Backscattering modulator, chipless RFID, radar cross section (RCS), small antennas, ultra-wideband (UWB).

1 Introduction

The signal reflected back, or backscattered, by RFID cards carries not only coded data used for card recognition, but it also contains relevant information about attached antenna properties [1]. Backscattering methods are therefore widely used for measuring the radiation pattern of RFID antennas based on a specific parameter named radar cross section (RCS). Because the interrogation and reading of a RFID device can take place from any direction, low directivity is therefore a mandatory property of the small RFID antennas. This means that the antennas radiation pattern is influenced by any object positioned in their near-field region, so free-space radiation conditions are mandatory for accurate measurement [2] - [4].

Inverse proportionality relationship between dimensions and quality factor of an antenna leads to large quality factors, i.e. highly reactive input impedances [5]. This characteristic is associated with narrow bandwidths and lower efficiency, due to near-field diffraction and propagation along cables, impedance matching networks and signal feeding structures with baluns (for balanced antennas).

Novel chipless RFID cards based on multiple resonant circuits [6], [7] and future sensing applications of the acoustic wave resonators working at frequencies over 5 GHz [8] demand antennas with 50 Ω input impedance. This condition is more stringent for chipless cards since, in case of a large bit number, the resonators may cover full ultra-wideband (UWB) frequency range (3.1 – 10.6 GHz) with specific radio regulations [9], [10].

Another relevant aspect of small antenna characterization is related to the efficiency of wireless energy harvesting over broad frequency ranges. This operating parameter is limited by antennas input impedance vs. input impedance of the harvesting circuit, since regular RFID applications are narrowband. Therefore, alternate solutions have to be taken in consideration. Good efficiency in using this resource is important, because complex measurements take a very long time due to multiple frequencies, angle values, etc.

Currently, the backscattering modulators for narrowband RFID applications utilize CMOS transistors as two-state, variable load impedances, because they are extremely small and operate at low voltages. Also, light controlled photo-conductive switches or electro-optical and opto-electrical converters are easily integrated in backscattering modulators due to their small dimensions without perturbing the near-field region of the AUT. Still their efficiency is quite limited by poor values of the backscattered power [11], [12]. On the other hand, higher signal powers are available from RF oscillators attached to the AUT and biased from low profile battery cells. However, signals with constant frequency and stable power levels can be obtained from these circuits for very short periods of time [13].

Our alternate solution is a broadband backscattering modulator based on monolithic integrated circuits of single-pole double through (SPDT) category, presented in this paper [14]. The internal structures of most switch models allow components control by means of two-level, complementary signals of the same polarity [15]. They cover large bandwidths, suitable for UWB antennas. A good isolation between ports means that reflection coefficients of the modulator are uncorrelated one to each other, an useful feature in some applications [16]. The circuit is therefore customizable for large bandwidth applications compared with current RFID backscattering modulators. Moreover, the modulator features very low power consumption, required for high accuracy, long term measurements.

2 Broadband switching solutions

According to the dictionary definition [17], the switching circuit can (i) close (ON state) or open (OFF state) a single signal path, for single pole single throw (SPST) structures, or (ii) it diverts the signal energy from one part of the circuit to another one, in case of multiple signal paths. From the second category, single pole double throw (SPDT) switches are frequently used in RF applications.

The switching devices are therefore defined by two characteristic states, named ON and OFF, according to the rules applied to regular electrical switches. The electronic switch versions can be easily described by simple equivalent circuits, based on a few

parameters defined for their preliminary analysis: (i) a low value resistor if the signal passes (ON state, described by insertion loss), and (ii) a low capacitance for OFF state, or isolation parameter (the signal is blocked).

RFID backscattering modulators use single, low cost semiconductor devices as two-state switches for changing the load impedance seen by the RFID antenna. PIN diodes and most field effect transistor (FET) models with either junction or insulated gates[1] are extensively utilized in switching applications. Of these, the forward biased PIN diode is normally assimilated to a resistor R_F controlled by its bias current I_F as

$$R_F \sim k/I_F^x \tag{1}$$

where the factor k depends on certain technological and physical parameters of the device, and the exponent x has a value relatively close to unity [18]. Alternately, the diode presents a low capacitance C_d over a broad range of reverse bias voltages.

The channel of a FET can be also switched between (i) conduction (ON state), described by a low value resistor (transistors channel resistance R_{ds-ON}) and (ii) non-conducting (OFF) or cutoff state, equivalent with a very low capacitance (C_{ds-OFF}) of the blocked channel. The components associated with the transistor are defined with reference to its drain and source terminals.

The electrical characteristics of the SPDT switch presented in Figure 1.a can be analyzed with a simplified schematic diagram (Figure 1.b) with passive components replacing the active devices switched in ON/OFF states relative to a common RF port (RFC): the signal path in ON state is replaced by a low value series resistor, whereas the path in OFF state is replaced by a small value capacitor.

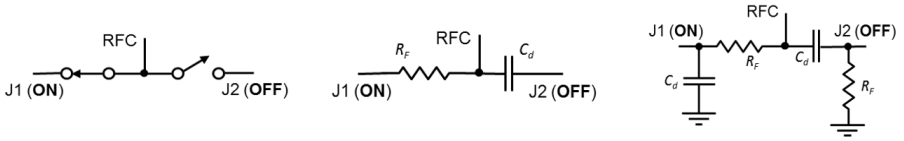

(a) (b) (c)

Fig. 1: SPDT switch: general electrical diagram representation (a), simplified schematic diagram with passive components (b), and circuit version with improved isolation (c).

The series resistance R_F is assumed frequency independent, hence the insertion loss during ON state is considered constant. On the other hand, the reactance of C_d is in inverse proportionality relationship with the operation frequency, therefore the isolation of an OFF capacitive section is reduced as more as frequency increases. This issue is normally solved by adding a second device at the output of each switched port, in parallel connection with it (Figure 1.c). While the ON state is not influenced too much by the low capacitance in shunt connection, the most significant effect occurs over OFF path, as the additional resistance at the output port in OFF state creates a low impedance path for the bypassed signal.

The simulation presented in Figure 2 compares the isolation of (i) a single series capacitor $C_d = 0.1$ pF (OFF path in Figure 1.b), and (ii) combination of the same series capacitor with $R_F = 2\Omega$ shunt resistor (OFF state branch in Figure 1.c).

[1] Insulated gate (e.g. MOS) transistors are also included in this category.

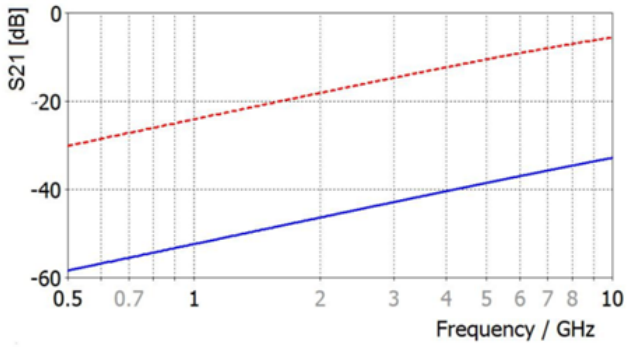

Fig. 2: Isolation provided by a single 0.1 pF series capacitor (dotted line) compared with isolation of 0.1 pF series capacitor and 2 Ω shunt resistor combination (continuous line).

More than 27 dB improvement of the isolation is therefore observed for the second circuit version at 10 GHz.

From the devices' point of view, both PIN diodes and FETs are excellent candidates for low power, broadband switching applications, since they have (i) quite similar electrical characteristics and (ii) are described by compatible equivalent circuits for either ON or OFF states (Figure 1). However, the PIN diode switches require (i) dual polarity power supplies for an efficient control, and (ii) the forward bias currents used for obtaining low resistance values are too large in order to be accepted in backscattering modulators.

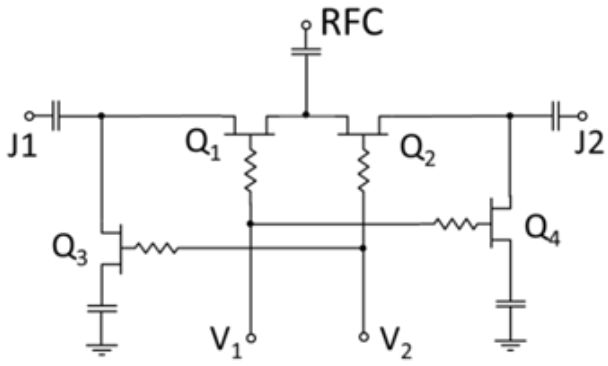

Fig. 3: Simplified schematic diagram of a MMIC SPDT switch with field effect transistors.

That is why microwave switches with FET-type devices are preferred for applications demanding very low power consumption due to their *voltage controlled* conduction. Certain integrated circuit switch models are also operated from single polarity control signals, a significant advantage for the majority of high volume wireless designs based also on single, positive voltage supplies. Good impedance matching and almost constant insertion loss and isolation are also specific for these components. Most electrical diagrams of this category of SPDT switches can be reduced to a simple model

(Figure 3), built according to Figure 1.c and based on series-shunt combinations of the active devices [19].

This switch model has a ground terminal; therefore any single-ended component can be connected to its ports. This aspect is important for UWB antennas which are normally fed by either coplanar (CPW) or microstrip transmission lines, both with reference ground planes. Due to this aspect, the radiation patterns are less influenced by closely placed objects as long as they are small enough.

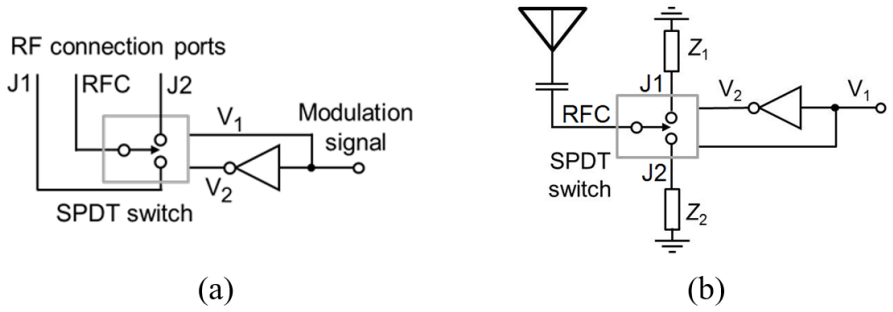

Fig. 4: Backscattering modulators with MMIC SPDT switches (a); load impedance connections in SPDT switch modulators for single ended antennas (b).

The circuit is controlled with logic-type complementary signals V_1 and V_2 available from a single signal source and an inverter gate (Figure 4.a). In case of backscattering applications, a single-ended antenna is always connected to the RFC port, whereas terminals J1 and J2 are loaded with complex impedances Z_1 and Z_2 (Figure 4.b) of the values selected according to the specific criteria detailed in the next section.

Table 2 presents the main electrical parameters and operating conditions for a selection of commercially available SPDT switches, with very low minimum operating frequencies, while the maximum operating frequency of some circuits starts from 4 GHz for AS186-302 switch [20], and increases over 10.6 GHz, mandatory for UWB applications [21], [22].

Table 1: Parameter comparison for three broadband SPDT switches.

No.	Parameter	Unit	AS186-302	TGS2352-2-SM	PE42520
1.	Bandwidth (typ.)	GHz	LF - 4	0.5 - 12	LF - 13
2.	Insertion loss	dB	1.25	1	2 (max.)
3.	Isolation[2]	dB	35 (min.)	35 (typ.)	18 (min.)

Despite of their outstanding characteristics (very low insertion loss and high isolation over extremely broad frequency bands), the operating conditions of the last two models are not compliant with usual RFID applications: large voltage and current levels for their bias or control signals, or dual power supplies.

[2]Minimum recommended values.

3 Antenna related radar cross section issues

The power budget in a wireless link described by a transmitter with P_{Tx} available input power and G_{Tx} antenna gain, and a receiver with G_{Rx} antenna gain and located at distance d from the transmitter antenna, is defined by the power at the receiving antenna port as [23]:

$$P_{Rx} = \frac{P_{Tx} \cdot G_{Tx} \cdot G_{Rx} \cdot \lambda^2}{(4\pi d^2)} \tag{2}$$

where λ is the wavelength corresponding to the operation frequency f. This relationship is valid for lossless connection cables, free propagation path, perfect alignment and full polarization match of the antennas.

The *scalar* RCS σ of a minimum scattering antenna with gain G, radiation resistance R_a, complex input impedance Z_a, and loaded with impedance Z_L is calculated from [24].

$$\sigma = \frac{\lambda^2 G^2 R_a^2}{\pi \mid Z_a + Z_L \mid^2} \tag{3}$$

A derived parameter, namely differential RCS ($\Delta\sigma$) [25], is preferred for this analysis:

$$\Delta\sigma = \frac{\pi^2 G^2}{4\pi} \mid \rho_1 - \rho_2 \mid^2 \tag{4}$$

where ρ_1, ρ_2 are the reflection coefficients corresponding to the load impedances for each state of the switch, i.e. Z_{L1} and Z_{L2}

$$\rho_{1,2} = (Z_{L1,2} - Z_a^*)/(Z_{L1,2} + Z_a) \tag{5}$$

In order to re-write (4) in a more compact way, normalized differential RCS ($\overline{\Delta\sigma}$) can be defined as

$$\overline{\Delta\sigma_{max}} = \frac{4\pi}{\lambda^2 G^2} \cdot \Delta\sigma = \mid \rho_1 - \rho_2 \mid^2 \tag{6}$$

The normalized differential RCS reaches its maximum value $\overline{\Delta\sigma_{max}} = 4$ if, for instance, $Z_{L1} \longrightarrow 0$ and $Z_{L2} \longrightarrow \infty$, or other reflection coefficients combination having unity amplitudes and $180°$C relative phase difference [25]. However, these impedance values are not easily implemented in broadband modulators, hence both load impedances are mainly selected for improving in-band RCS uniformity, rather than optimizing $\overline{\Delta\sigma}$. In fact, the optimization of $\overline{\Delta\sigma}$ is mostly relevant for *pure* RFID applications, because the tags' detection sensitivity is of primary importance. For the proposed measurement in a well controlled RF environment, the lack of sensitivity becomes critical only if the measured antenna has a radiation pattern with very large changes of the antenna gain.

A microstrip fed, single-ended UWB antenna was derived from an existing model [26], due to the reduced influence on its input impedance from the ground plane layout. Besides connectorized antenna version (Figure 5), used for regular characterization in transmit mode, the same antenna was integrated on a single substrate with the broadband SPDT switch modulator for the radiation pattern measurement based on backscattering methods.

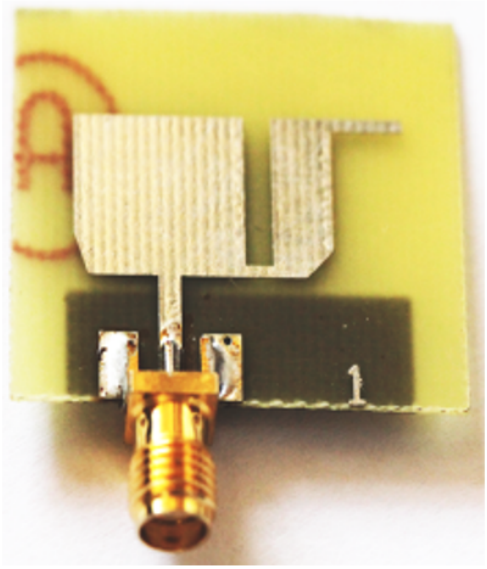

Fig. 5: Connectorized UWB antenna used for radiation pattern measurement.

Since the AUT is of UWB type, the assumption $Z_a \approx 50\,\Omega$ is considered valid over full antenna bandwidth. According to (5), the reflection coefficient's amplitude becomes $\mid \rho_1 \mid \longrightarrow 0$ if the load impedance is also $Z_1 = 50\,\Omega$. The second load impedance (Z_2) can be replaced with a purely reactive load for maximizing the differential RCS, since the amplitude of the reflection coefficient becomes $\mid \rho_2 \mid \longrightarrow 1$ over a broad frequency range. The reactance can be a small value capacitor, with much lower losses compared with regular RF inductors.

4 Experimental results

A novel bistatic antenna arrangement was presented in [14] for backscattering based radiation pattern measurement. The measurement protocol specifies that both interrogation antenna (TxA) and AUT are held in stationary positions until the measurement procedure is completed, while the third antenna (RxA), in receiving mode, turns on circular trajectories around AUT and points to it (Figure 6).

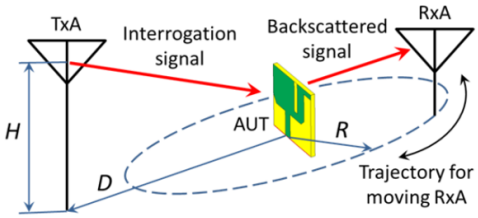

Fig. 6: Connectorized UWB antenna used for radiation pattern measurement.

Excellent accuracy of the proposed measurement procedure is therefore expected, as the coupling factor between TxA and AUT remains unchanged. Distance D from AUT to TxA, height H of TxA, and radius R of receiving antenna (RxA) trajectory are selected for avoiding any obstruction within signal paths. For AUT's radiation pattern measurement, a high performance reflection-type broadband backscattering modulator, acting on amplitude and/or phase of the incident signal, was proposed. The reflected RF signal is spread out into space according to the three-dimension (3-D) radiation pattern of the AUT [1].

Due to the measurement system's inherent accuracy stated above, it can be considered that only changes in the electrical parameters of the backscattering modulator can influence the measurement results. An investigation of reflection coefficients alteration as a result of control voltage uncertainty over long measurement sessions was therefore performed. The actual UWB modulator is based on an AS186-302 SPDT monolithic integrated switch [20].

Table 2: Power supply voltage and control signal amplitude of the active components.

IC type	**Power supply or control voltage**
AS186-302 SPDT switch	3 V (min.)
Ultra High Speed CMOS family	1.65 – 5.5 V
SG-3040JC CMOS quartz oscillator	1.8 – 3.6 V

CR2032 button cell batteries [27] are widely used for memory back-up, remote controls, home appliances, and other low power circuits. According to the power supply and control voltage requirements of the backscattering modulator (Table 3), a single CR2032 element is suitable for our application, due to its specification:

- 3.0 V nominal voltage (maximum open circuit voltage - OCV: 3.7 V);
- 200 mAh capacity (typical value);
- nominal dimensions: 20 mm diameter, and 3.2 mm height.

In order to have reliable information about the voltage stability over a long period of time for this battery, the backscattering modulator was permanently connected to it and its output voltage was periodically measured.

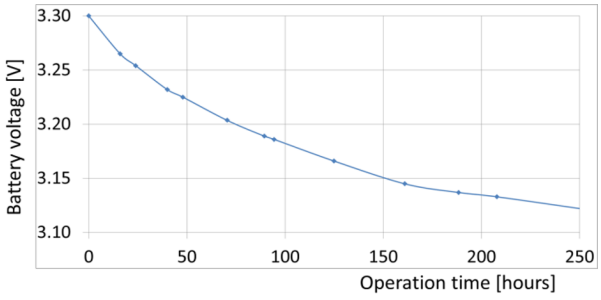

Fig. 7: CR2032 battery voltage vs. operating time with actual loading conditions.

An average value of 20.7 mV/day voltage drop was therefore calculated from the actual result presented in (Figure 7) and obtained during a 10 day data acquisition

interval. A current consumption of only 3.5 μA, measured for the complete modulator, explains this outstanding result. The low frequency (32.768 kHz) quartz oscillator model SG-3040JC [28] was also selected for its low power consumption, because higher frequency oscillators need larger bias currents.

Although the SPDT switch is specified for 4 GHz maximum operating frequency, it was measured with very good results up to 6 GHz, obtaining an input-to-output isolation better than 28 dB, and maximum insertion loss of 2 dB up to 5.6 GHz and 3 dB at 6 GHz (Figure 8).

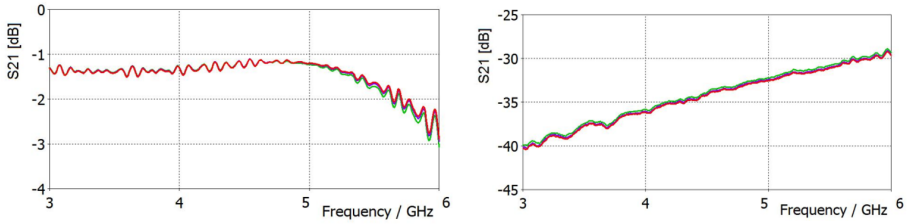

Fig. 8: Insertion loss (a) and isolation (b) of the AS186-302 SPDT switch measured at 2.5 V, 3 V, and 3.5 V control voltage amplitudes.

These results were measured with 37397D vector network analyzer for three amplitudes of the control voltages (2.5 V, 3 V and 3.5 V) because a certain voltage drop is expected from the battery used as modulator's power supply. It can be easily observed that all three traces are almost superposed: in fact, the changes are less than 0.17 dB for insertion loss and about 0.35 dB in case of isolation. Excellent stability of the electrical parameters can be therefore achieved with this device, even outside of its recommended operation conditions.

Because the power supply voltage is not stable during long measurement sessions of the backscattering modulator, the effect of actual bias conditions on reflection coefficients and normalized differential RCS were required.

The reflection coefficients were also measured at the antenna port of the "reference" modulator, using the following experimental conditions: the actual impedances Z_1 and Z_2 loading the backscattering modulator and all three control voltages mentioned above. Some of the new scattering parameter sets (*.s2p files in Touchstone format) contain direct information about the reflection coefficients change as a result of control voltage drop. As a direct result, an average value of 0.02 dB/day change in the magnitude of ρ_1 reflection coefficient was noticed, while the magnitude of ρ_2 remained almost constant

Table 3: Reflection coefficients and normalized differential RCS vs. control voltages.

V1, V2	ρ_1 (magnitude/angle)	ρ_2 (magnitude/angle)	$\overline{\Delta\sigma}$
2.5 V	$0.220/-119.8°$	$0.836/-252.9°$	0.689
3.0 V	$0.206/-118.1°$	$0.835/-252.4°$	0.698
3.5 V	$0.197/-116.6°$	$0.835/-251.9°$	0.704

Table 3 summarizes the normalized differential RCS results, calculated from modulators reflection coefficients (all control voltages taken into account) and AUT input

impedance $\underline{Z_a}$, which is completely independent on any external condition. In this way, about $\overline{\Delta\sigma}$ = 0.004 dB/day average change of normalized differential RCS results. All values mentioned above confirm that long measurement sessions can be performed with negligible errors from the power supply drop off.

A version of the antenna shown in (Figure 5) was loaded, without coupling connectors, by the backscattering modulator based on MMIC SPDT switch. The radiation pattern of this antenna was measured using the bistatic setup described above.

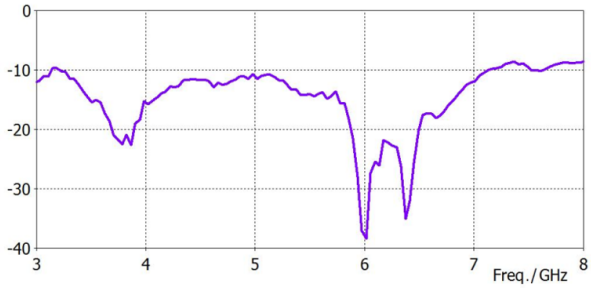

Fig. 9: Experimental reflection coefficient of the connectorized AUT.

As one can see from the connectorized antenna measurement (Fig. 9), the actual frequency range for a reflection coefficient better than – 10 dB is about 3.2 – 7.2 GHz. This result permits the use of the UWB antenna for low power applications over 5 GHz band, including wireless reading of SAW resonator sensors [8].

The antenna provided with the complete backscattering modulator was manufactured on a double-sided printed circuit board (PCB) with 30×35 mm^2 area Figure 10. The same FR-4 substrate was used for both connectorized UWB antenna and its test version. A relatively thin substrate (0.8 mm) was considered in our application, due to reduced parasitic radiation at high frequencies and dimensional compatibility with low pitch SMD components.

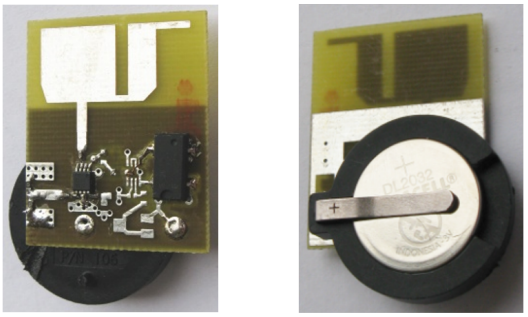

(a) (b)

Fig. 10: Assembled backscattering modulator: AUT side view (a), and ground plane side view (b).

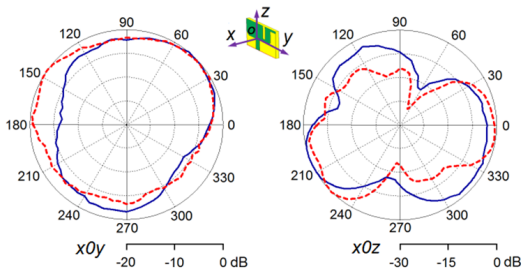

(a) (b)

Fig. 11: Normalized radiation patterns measured with AUT in transmit mode (dotted lines) and using proposed backscattering method (continuous lines).

The backscattering modulator is made of active components (SPDT switch, CMOS inverter, quartz oscillator) and several passive devices (switched load impedances, timing and decoupling capacitors) including the tiny battery with its support.

Using the proposed bistatic setup, the radiation patterns of the AUT integrated with the backscattering modulator was measured at 5.5 GHz. This frequency was selected because both TxA and RxA high gain antennas have a limited bandwidth centered near 5.5 GHz. The results are compared in Figure 11 with the equivalent radiation patterns measured for connectorized antenna in transmission mode, hence influenced by the coaxial cable used for RF feeding signal [14]. The traces are normalized to their maximum values, for an easier comparison. Although the radiation patterns look quite similar in each plane, differences up to 8 dB are observed in some directions, mainly due to different radiation conditions in the surrounding environment.

5 Conclusions

A novel wide bandwidth amplitude modulator based on single-pole double through integrated switches has been designed for accurate measuring the radiation pattern of UWB small antennas using backscattering methods. The circuit is extremely flexible regarding reflection coefficients presented to the AUT, and supports very large bandwidths. The bistatic configuration of the antennas used in radiation pattern measurements provides excellent accuracy due to constant irradiation of the AUT from the interrogation antenna. The backscattering modulator was designed and manufactured with commercially available components. Due to 3.5 μA current consumption of the modulator, the reflection coefficients' amplitude changed about 0.02 dB/day for ρ_2 or it remained almost constant for ρ_2, so an error on differential RCS less than = 0.004 dB/day was obtained.

Acknowledgements. The authors acknowledge the support of the EC under Integrated FP7 Project SMARTPOWER (FP7 Grant agreement no.288801/2011-2016).

References

[1] APPEL-HANSEN J., *Accurate determination of gain and radiation patterns by radar cross-section measurements*, IEEE Trans. Antennas Propag., vol. 27, no. 5, Sep. 1979, pp. 640-646, doi: 10.1109/TAP.1979.1142156

[2] PURSULA P., HIRVONEN M., JAAKKOLA K., VARPULA T., *Antenna effective aperture measurement with backscattering modulation*, IEEE Trans. Antennas Propag., vol. 55, no. 10, Oct. 2007, pp. 2836-2843, doi: 10.1109/TAP.2007.905821

[3] BORIES S., HACHEMI M., HAJ KHLIFA K., DELAVEAU C., *Small antennas impedance and gain characterization using backscattering measurements*, 2010 Proc. of the Fourth European Conf. on Antennas and Propagation (EuCAP), pp. 1-5, Barcelona, Spain, ISBN 978-1-4244-6431-9 (print)

[4] MAYER L. W., SCHOLTZ A., *Efficiency measurement method for UHF transponder antennas*, First Int. EURASIP Workshop on RFID Technology, Sept. 2007, pp. 1720

[5] MCLEAN J. S., *A re-examination of the fundamental limits on the radiation Q of electrically small antennas*, IEEE Trans. Antennas Propag., vol. 44, no. 5, May 1996, pp. 672-676, doi: 10.1109/8.496253

[6] S. Preradovic, N.M. Karmakar, *Chipless RFID: bar code of the future*, Microw. Magazine, vol. 11, no. 7, Dec. 2010, pp. 87-97, doi: 10.1109/MMM.2010.938571

[7] PRERADOVIC S., KARMAKAR N., *Chipless millimeter wave identification (MMID) tag at 30 GHz*, 978-2-87487-022-4 2011 EuMA 10-13 October 2011, Manchester, UK, pp. 123-126, ISBN 978-1-61284-235-6 (print)

[8] MLLER A., KONSTANTINIDIS G., BUICULESCU V., DINESCU A., STAVRINIDIS A., TEFNESCU A., STAVRINIDIS G., GIANGU I., CISMARU A., MOLDOVEANU A., *GaN/Si based single SAW resonator temperature sensor operating in the GHz frequency range*, Sensors and Actuators A: Physical, vol. 209, pp. 115-123, 2014, doi: 10.1016/j.sna.2014.01.028

[9] *** ETSI TR 103181-3, v1.1.1 (2016-08) Short Range Devices (SRD) using Ultra Wide Band (UWB); Part 3: Worldwide UWB regulations between 3.1 and 10.6 GHz

[10] *** FCC: Title 47 (Telecommunication), Section 15 (Radio Frequency Devices) of the Code of Federal Regulations (subpart F - UWB)

[11] YANAKIEV B., NIELSEN J. ., CHRISTENSEN M., PEDERSEN G. F., *Small device for short-range antenna measurements using optics*, IEEE Antennas Propag. Mag., vol. 53 , no. 6, pp. 148-152, Dec. 2011, doi: 10.1109/MAP.2011.6157732

[12] CANT H. I., IRONSIDE C. N., KELLY A. E., ROMEIRA B., FIGUEIREDO J. M. L., *An optical to wireless data link using radio frequency backscatter*, IEEE Microw. Wireless Compon. Lett., vol. 23, no. 2, pp. 102-104, Feb. 2013, doi: 10.1109/LMWC.2013.2239983

[13] MAYER L. W., SCHOLTZ A. L., *Gain and input impedance measurement for UHF transponder antennas*, Proc. Int. Symp. on Antennas and Propagation, ISAP 2008, Taipei, Taiwan

[14] BUICULESCU V. GIANGU I., *Backscattering modulators with flexible impedance loading for radiation pattern measurement of small, broadband antennas*, Proc. 39th Intl. Semiconductor Conference - CAS-2016, Sinaia, Romania, pp. 75-78, 2016, doi: 10.1109/SMICND.2016.7783043

[15] http://www.skyworksinc.com/uploads/documents/200363A.pdf, APN2017 application note

[16] BLETSAS A., DIMITRIOU A. G., SAHALOS J. N., *Improving backscatter radio tag efficiency*, IEEE Trans. Microw. Theory Tech., vol. 58, no. 6, June 2010, pp. 1502-1509, doi: 10.1109/TMTT.2010.2047916

[17] http://www.dictionary.com/browse/switch?s=t

[18] *** "*The PIN diode circuit designers handbook*", Microsemi Corp., 1998

[19] DONG M., *Analyze transient delays in GaAs MMIC switches*, Microwaves & RF, Feb. 2017, pp. 56-58, 60-62

[20] http://www.skyworksinc.com/uploads/documents/200104D.pdf, AS186-302LF data sheet

[21] Available online at http://www.triquint.com/products/p/TGS2352-2-SM

[22] Available online at http://www.psemi.com/pdf/datasheets/pe42520ds.pdf

[23] BALANIS C. A., Antenna theory: analysis and design, John Wiley & Sons, 1997

[24] NIKITIN P. V., RAO K. V. S., *Theory and Measurement of Backscattering from RFID Tags*, IEEE Antennas Propag. Mag., vol. 48, no. 6, Dec. 2006, pp. 212-218, doi: 10.1109/MAP.2006.323323

[25] NIKITIN P. V., RAO K. V. S., MARTINEZ R. D., *Differential RCS of RFID tag*, Electron. Lett., 2007, vol. 43, no. 8, pp. 431-432, doi: 10.1049/el:20070253

[26] CHEN Z.N., SEE T.S.P., Qing X., *Small printed ultrawideband antenna with reduced ground plane effect*, IEEE Trans. Antennas Propag., vol. 55, no. 2, Feb. 2007, pp. 383-388, doi: 10.1109/TAP.2006.889823

[27] http://image.sciencenet.cn/olddata/kexue.com.cn/bbs/upload/15791IEC60086-2_%7B10%5B1%5D%5B1%5D.1%7D%282001-10%29.pdf

[28] http://www.epsondevice.com/docs/qd/en/DownloadServlet?id=ID000648